

LIDAR DETERMINATION OF QUARTZ CONCENTRATION IN THE TROPOSPHERIC MINERAL AEROSOLS – METHODOLOGY AND FIRST RESULTS

Boyan Tatarov^{(1),(2)}, Nobuo Sugimoto⁽¹⁾, Ichiro Matsui⁽¹⁾

⁽¹⁾ National Institute for Environmental Studies, 16-2 Onogawa, Tsukuba, Ibaraki 305-0053, Japan,
E-mail: boyan.tatarov@nies.go.jp

⁽²⁾ Institute of Electronics, Bulgarian Academy of Sciences, 72 Tsarigradsko Shosse Blvd., Sofia 1784, Bulgaria

ABSTRACT

This paper presents a lidar method that enables the determination of quartz concentration in mineral aerosols from simultaneously measured, high-spectral-resolution lidar and quartz Raman lidar signals. The method and experimental results are presented.

1. INTRODUCTION

The mineral aerosol injected into the atmosphere over desert areas has significant effects on the Earth's radiative budget as well as on the environment and ecology. Assessment of the impact of mineral aerosols on climate and the environment requires specific knowledge of the temporal and spatial distribution and the optical properties of the aerosols.

Over the past years, lidars (light detection and ranging systems) have become powerful tools for aerosol observations. Mie scattering lidars capable of measuring depolarization are useful for monitoring aerosol distributions. Using the depolarization ratio measurements, one can estimate dust aerosol distributions based on simple assumptions [1]. However, Mie lidars have limitations in the quantitative derivation of aerosol optical parameters. Multi-wavelength lidars can provide additional information on aerosol characterization, but they also require simplified assumptions in the data analysis. High-spectral-resolution lidars (HSRL) [2,3] and Raman lidars [4] both enable independent quantitative measurements of the aerosol backscatter and extinction coefficient profiles. The lidar ratio consequently obtained is useful for characterizing aerosols and ice clouds. However, it is still not possible to estimate mineral dust concentration in an aerosol mixture without simple assumptions, even if one combines HSRL and the depolarization ratio measurement.

In this work, we present a method using Raman scattering of quartz (silicon dioxide, silica), which is the major constituent of mineral dust. This method combines the Raman lidar using a 466 cm⁻¹ quartz line with an HSRL to estimate the quartz concentration in the atmospheric aerosols.

2. METHODOLOGY

There are two reasons to select quartz as a tracer for detecting mineral aerosol. The first is the high relative

concentration of quartz in mineral aerosols. In particular, for aerosols generated in Asian deserts [5], approximately 46-77% of particles are Si-rich particles primarily composed of quartz and aluminosilicate. The second reason is that the quartz Raman line at 466 cm⁻¹ is suitable for lidar measurements. Commercial filters can easily separate this line from the Mie scattering signal, Doppler-broadened molecular signal, and Raman lines of other atmospheric components [6], such as N₂ at 2330 cm⁻¹, O₂ at 1556 cm⁻¹, O₃ at 1103 cm⁻¹, CO₂ at 1388 cm⁻¹, and water vapor at 3652 cm⁻¹.

The Raman backscatter signal is described by the so-called Raman lidar equation and can be written as [4]:

$$P_R(r, \lambda_L, \lambda_R) = P_L \frac{B_R F_R(r)}{r^2} \beta_R(r, \lambda_L, \lambda_R) \times \exp\left(-\int_0^r [\alpha_p(z, \lambda_L) + \alpha_m(z, \lambda_L) + \alpha_p(z, \lambda_R) + \alpha_m(z, \lambda_R)] dz\right) \quad (1),$$

where $P_R(r, \lambda_L, \lambda_R)$ is the power received from distance r at the Raman wavelength λ_R , P_L and λ_L are the power and wavelength of transmitted light, $F(r)$ is the geometrical form factor of the transmitter/receiver system, B is a constant including all range independent parameters, and $\beta_R(r, \lambda_L, \lambda_R)$ is the Raman backscatter coefficient. The extinction coefficients are denoted by α_p for aerosol particles and α_m for atmospheric gaseous molecules.

The Raman backscatter coefficient $\beta_R(r, \lambda_L, \lambda_R)$ of the scatters (silicon dioxide in our case) can be determined from the received Raman scattering signal based on knowledge of system parameters (B and $F(r)$) and the optical depth of the atmosphere. While the geometrical form factor and the efficiency of the system can be calculated or determined by calibration measurements, additional assumptions or independent measurements are required to determine the optical depth. Aerosol extinction and backscatter coefficients at the laser wavelength are obtained by simultaneous HSRL observation. Detailed descriptions of HSRL principles and methods are found in [2,3,7]. A Raman scattering lidar for nitrogen or oxygen can also provide aerosol backscatter and optical depth profiles.

To solve the Raman scattering equation (Eq. 1), the air molecular extinction $\alpha_m(r, \lambda_L)$ and backscatter $\beta_m(r, \lambda_L)$ profiles as well as the particle extinction coefficient at Raman wavelength must be known. Atmospheric molecules scattering profiles can be obtained from model data or from the temperature and pressure profiles derived from standard meteorological measurements. The aerosol extinction profile at the Raman wavelength can be obtained from the aerosol extinction profile at the laser wavelength by assuming power-law wavelength dependence [4].

In this manner, one can obtain a solution of the Raman equation (Eq. 1) with respect to the Raman backscatter coefficient for quartz as follows:

$$\beta_R(r, \lambda_L, \lambda_R) = \xi(r) \frac{P_R(r, \lambda_L, \lambda_R)}{P_m(r, \lambda_L)} \times \beta_m(r, \lambda_L) \eta(r, \lambda_L, \lambda_R) \quad (2),$$

where $\xi(r)$ is the ratio of the system parameters of the Raman and molecular channels of the lidar, $P_m(r, \lambda_L)$ is the received power from air molecule backscattering produced by HSRL (which is attenuated by air and aerosol extinction), and $\eta(r, \lambda_L, \lambda_R)$ is the correction factor for the dependence of the optical depth on wavelength.

The mass concentration of silica in the atmosphere can be estimated based on the Raman backscatter coefficient for quartz. The relation of the Raman backscatter coefficient with the Raman backscatter differential cross section $d\sigma(\lambda_L, \lambda_R, \pi)/d\Omega$ and the number density of quartz molecules N_q can be used for this purpose. The relation is defined by the expression:

$$\beta_R(r, \lambda_L, \lambda_R) = N_q(r) \frac{d\sigma(\lambda_L, \lambda_R, \pi)}{d\Omega}. \quad (3)$$

Using this equation (Eq.3), one can estimate the number density and then mass concentration if the differential cross section is known. The absolute value of the Raman differential cross section in the backscatter direction of natural quartz is significantly dependent on the structure of the crystal (alpha-quartz, beta-quartz, alpha-, beta1-, and beta2-tridymite, alpha- and beta-cristobalite), the crystallization process and the presence of amorphous silica, and the conditions of admixtures. This makes it difficult to derive the differential cross section for quartz in mineral dust particles. Thus far, we have not been able to find the differential cross section obtained by laboratory experiment on mineral dust in our available bibliography. Here, we use 3.8×10^{-30}

$\text{cm}^2 \text{sr}^{-1} \text{molecule}^{-1}$ at 466 cm^{-1} reported by Schoen and Cummins as the value of the cross section [8].

3. LIDAR EQUIPMENT

The method developed has been applied to the experimental data obtained by the HSRL at the National Institute for Environmental Studies (NIES) [7]. The lidar system was modified with one additional channel to enhance the reliability of quartz detection. The wavelength $\lambda_L=532.24 \text{ nm}$ ($18788.451 \text{ cm}^{-1}$) was chosen for the HSRL measurements. The excitation of the silicon dioxide molecules by this wavelength yielded a scattered radiation with a wavelength $\lambda_R=545.8 \text{ nm}$ for the Raman line at 466 cm^{-1} . Initially, two commercial filters were used to take reliable measurements of the Raman-shifted return. The first is a ‘‘Raman edge filter’’ (CVI, REF-532.0-A) characterized by an optical density of about 10 for the laser line ($\lambda_R=532.24 \text{ nm}$) and an averaged pass-band transmission of more than 93% for wavelengths from 537 nm to 736 nm. The second is an interference filter (CVI, F03-546.1-4-2.00) with a center wavelength of 546.1 nm and bandwidth of 3 nm (FWHM). The blocking optical density at the laser wavelength is close to 5. Subsequently, to increase the rejection ratio a supplementary ‘‘Raman edge filter’’ (CVI, REF-532.0-A) was added. In the current design of the receiver, the transmission at the laser wavelength is 25 to 26 orders of magnitude smaller than that for the quartz Raman signals.

Numbers of tests of optical rejection were carried out under clean-air conditions using an additional interference filter with a center wavelength of 532 nm. As the result, no elastic scattering signals were observed in the Raman channel above the noise level, including scattering from very dense water clouds. A principal systematic error can be due to presence of fluorescence from atmospheric component at wavelength of 546.1 nm. Additional error source is pure rotational Raman scattering which can be detected by the Raman quartz channel, because the wavelength shift of quartz Raman scattering is only 12 nm. The ratio of the system parameters $\xi(r)$ was determined from the factory data of the filters and the calibration measurement without the filters. A value of the power exponent $k=1$ was used for calculating of the correction factor $\eta(r, \lambda_L, \lambda_R)$.

4. RESULTS

Figure 1 presents an example of data obtained on April 30, 2005, using the combination of the quartz Raman lidar and HSRL. The lidar system was located at NIES, Tsukuba, Japan (36.05 N, 140.12 E). The molecular optical profiles were obtained from the routine

radiosonde observations at Tateno Aerological observatory (36.05 N, 140.13 E). A large mineral dust plume had been transported over the lidar site on this day. The presence of the dust plume over this part of Japan was confirmed by independent measurements using polarization lidars in the NIES Lidar Network [1] (Tsukuba (36.05 N, 140.12 E), Toyama (36.70 N, 137.10 E), and Matsue (35.21 N, 133.01 E)).

The vertical profiles of range-corrected lidar signals, particle backscatter (β_p) coefficient, Raman backscatter coefficient for quartz (β_R) calculated by eq. 2, and lidar ratio (S_p) are plotted in Fig. 1. Lidar signals were recorded from 1530 to 1630 UTC. The vertical resolution is 152 m.

In the profiles of range-corrected lidar signals (Fig. 1a), one can see the presence of several aerosol layers up to 5 km altitude with relatively high aerosol concentration

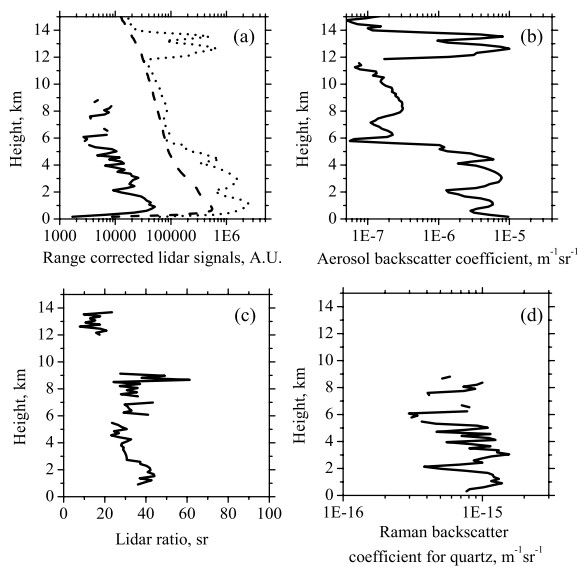


Fig. 1. Vertical profiles of optical properties obtained on 30 April 2005. (a) Range-corrected lidar signals: quartz scattering (solid), Rayleigh scattering (dashed), and combined Mie and Rayleigh scattering (dotted). (b) Aerosol backscatter coefficient. (c) Lidar ratio. (d) Backscatter coefficient due to Raman scattering.

and an additional thin layer between 6 km and 11 km. An ice cloud with a cloud base of 12 km to 14 km is also seen in the same graph. The Raman lidar signal indicates the presence of quartz for altitudes up to 6 km. Note that Raman signals are seen only in the ranges where quartz is present. Signals are not observed in the Raman channel from the ranges of the ice cloud. This indicates that there was no optical and electrical “cross talk” in the Raman channel.

The aerosol backscatter coefficient in the low aerosol layers was $\beta_p \sim 1 \times 10^{-6} \text{ m}^{-1} \text{ sr}^{-1}$ to $\beta_p \sim 8 \times 10^{-6} \text{ m}^{-1} \text{ sr}^{-1}$

(Fig. 1b). The lidar ratio (extinction-to-backscatter ratio) was about 40 sr at altitudes of 1 to 2.5 km and about 30 sr between 2.5 km and 5 km. The values are typical for dust aerosols. The lidar ratio in the elevated cirrus cloud was 15 sr, significantly different from that in the low altitude dust layer. The profile of the Raman backscatter coefficient for quartz ($\beta_R(r)$) shown in Fig. 1d is similar to the aerosol elastic backscatter profile. It can be concluded that quartz (i.e. mineral dust) was the dominant constituent in the observed aerosol layer. These results are in good agreement with the Tsukuba lidar in the NIES Lidar Network, which observed a depolarization ratio of about 30% and a similar value for the particle backscatter coefficient from the aerosol layer at the same time. The averaged value of the Raman backscatter coefficient for quartz up to 5 km is about $9 \times 10^{-16} \text{ m}^{-1} \text{ sr}^{-1}$. Using the value of the differential cross section $3.8 \times 10^{-30} \text{ cm}^2 \text{ sr}^{-1} \text{ molecule}^{-1}$ and the observed Raman backscatter coefficient for quartz of $\beta_R = 9 \times 10^{-16} \text{ m}^{-1} \text{ sr}^{-1}$, one can estimate the number density of scatters to be $N_q = 2.3 \times 10^{11} \text{ molecules cm}^{-3}$ with eq. 3. Multiplying the molecular mass of silicon dioxide, $M(\text{SiO}_2) \approx 1 \times 10^{-24} \text{ g}$, the mass concentration of silicon dioxide is estimated to be $23 \mu\text{g m}^{-3}$. Using the extinction coefficient ($\alpha_p \sim 2.4 \times 10^{-4} \text{ m}^{-1}$) and the typical value of mass/extinction factor [1] for the region, $2 \times 10^5 \mu\text{g m}^{-3} \text{ m}^{-1}$, the mass concentration of all dust components is calculated to be $48 \mu\text{g m}^{-3}$. One can see that presented quartz mass concentration values have the same magnitude. The estimated value of quartz mass concentration is reasonable, but it is not a rigorous estimate because of the oversimplified assumptions. Accurate estimation of quartz mass concentration requires a systematic investigation of Raman scattering from desert dust samples.

Figure 2 presents an experimental result that demonstrates simultaneous measurement of Raman quartz scattering and the polarization characteristics. The vertical profiles of range-corrected lidar signals, particle backscatter (β_p) and extinction (α_p) coefficients, Raman backscatter coefficient for quartz (β_R), and lidar ratio (S_p), total (δ_t) and particle (δ_p) depolarization ratios are plotted in Fig. 2. The total depolarization ratio was defined as the ratio of the lidar signal with perpendicular polarization to that with parallel polarization, with respect to the polarization of the transmitted laser. The particle depolarization ratio is estimated from the δ_p , and backscattering ratio [1]. The δ_t is a more appropriate index for characterizing sphericity of particles, because it does not depend on the density of aerosol. Lidar signals were recorded from 1100 to 1200 UTC on 11 March, 2006. The vertical resolution is 152 m.

The vertical profiles of range-corrected lidar signal shows presence of two aerosol layers – first one up to

3.5 km altitude, and second from 4 km to 6.5 km. The Raman signal clearly indicates presence of quartz in the both layers. In the low layer, the extinction and backscatter coefficients were approximately $\beta_p \sim 2 \times 10^{-6} \text{ m}^{-1} \text{ sr}^{-1}$ and $\alpha_p \sim 1 \times 10^{-4} \text{ m}^{-1} \text{ sr}^{-1}$. The lidar ratio was in the range from 60 sr to 75 sr. The values of the extinction and backscatter coefficients were similar in the higher aerosol layer, but the lidar ratio on scatters around a mean value of 40 sr. This fact indicates a difference in microphysical characteristics of the particles. The averaged values of the Raman backscatter coefficient for quartz are $2.6 \times 10^{-16} \text{ m}^{-1} \text{ sr}^{-1}$ in altitudes up to 3.5 km and $4.9 \times 10^{-16} \text{ m}^{-1} \text{ sr}^{-1}$ from 4 km to 7 km. The mass concentrations of silicon dioxide are estimated to be $7 \mu\text{g m}^{-3}$ and $13 \mu\text{g m}^{-3}$, respectively.

The vertical profile of total depolarization ratio (Fig. 2c) has relative high values in the both layers (up to 10 % at 3 km, and up to 15 % at 5 km), which corresponds to scattering from particles with non-spherical shape. The higher values of depolarization ratio are observed in the same altitudes where Raman scattering from quartz is

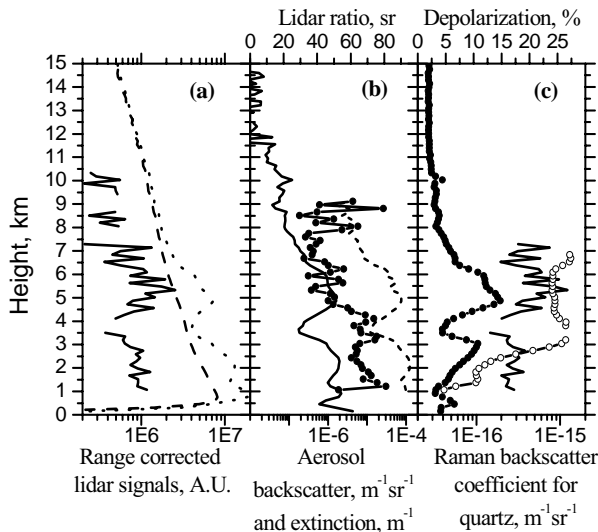


Fig. 2. Vertical profiles of optical properties obtained on 11 March 2006. (a) Range-corrected lidar signals: quartz scattering (solid), Rayleigh scattering (dashed), and combined Mie and Rayleigh scattering (dotted). (b) Aerosol backscatter (solid) and extinction (dotted) coefficients, Lidar ratio (circle). (c) Backscatter coefficient due to Raman scattering (solid), total (solid circle) and particle (open circle) depolarization ratios.

detected. The profile of particle depolarization ratio shows different behavior in the two aerosol layers. It is near to a constant value of 25 % in the upper layer, and it increases rapidly from 5 % to 25 % in the lower layer. In contrast, the Raman backscattering coefficient for quartz is almost constant. The reason for that difference is the presence of spherical aerosols at altitudes near to the ground. The higher values of the lidar ratio (about

70 sr) and the high relative humidity (more than 80%) measured by radiosonde at the lower aerosol layer support the explanation. The results show the significant advantage of the present method over the polarization approach for detecting mineral aerosols, especially in the mixture of spherical and nonspherical aerosols.

5. CONCLUSIONS

Simultaneous Raman lidar and HSRL measurements detected the presence of silicon dioxide, and mapped the vertical profile of mineral dust aerosols. The presented method, combined with future research on the optical constants of mineral dust, will enable quantitative lidar retrievals of quartz mass concentrations in the atmosphere. This approach will be useful for characterizing atmospheric aerosols and investigations of mineral dust. It will be especially useful for distinguishing dust and ice clouds in studies on the effect of dust particles as ice cloud nuclei.

REFERENCE

1. Shimizu, A., et al. Continuous observations of Asian dust and other aerosols by polarization lidar in China and Japan during ACE-Asia, *J. Geophys. Res.*, **109**, (D19) S17, 2004.
2. Shimizu, H., et al. High spectral resolution lidar system with atomic blocking filters for measuring atmospheric parameters, *Appl. Opt.* **22**, 1373, 1983.
3. Piironen, P. and E. W. Eloranta, Demonstration of a High-Spectral-Resolution Lidar based on a Iodine Absorption Filter, *Opt. Lett.* **19**, 234, 1994.
4. Ansmann, A., et al., Measurement of atmospheric aerosol extinction profiles with a Raman lidar, *Opt. Lett.* **15**, 746, 1990.
5. D. Trochkin, et al., Comparison of the chemical composition of mineral particles collected in Dunhuang, China and those collected in the free troposphere over Japan: possible chemical modification during long-range transport, *Water, Air, and Soil Pollution* **3**, 161, 2003.
6. Measures, R. M., *Laser Remote Sensing*, John Wiley, New York, 1984.
7. Liu, Z., et al. High-spectral-resolution lidar using an iodine absorption filter for atmospheric measurements, *Opt. Eng.* **38**, 1661, 1999.
8. P.E.Schoen and H.Z.Cummins, Absolute cross sections for Raman and Brillouin light scattering in quartz, *Proceedings of Second International Conference on Light Scattering in Solids*, M. Balkanski, ed., Flammarion, Paris, 460, 1971.